entropy

Article

Twisted Soft Photon Hair Implants on Black Holes

Fabrizio Tamburini [1,2], Mariafelicia De Laurentis [3,4,5,6], Ignazio Licata [7,8,9] and Bo Thidé [10,*]

1 ZKM—Zentrum für Kunst und Medientechnologie, Lorentzstr. 19, D-76135 Karlsruhe, Germany; fabrizio.tamburini@gmail.com
2 MSC-BW, Stuttgart, Nobelstr. 19, 70550 Stuttgart, Germany
3 Institute for Theoretical Physics, Goethe University, Max-von-Laue-Str. 1, D-60438 Frankfurt, Germany; laurentis@th.physik.uni-frankfurt.de
4 Tomsk State Pedagogical University, ul. Kievskaya, 60, 634061 Tomsk, Russia
5 Laboratory of Theoretical Cosmology, Tomsk State University of Control Systems and Radioelectronics (TUSUR), 634050 Tomsk, Russia
6 INFN Sezione di Napoli, Compl. Univ. di Monte S. Angelo, Edificio G, Via Cinthia, I-80126 Napoli, Italy
7 Institute for Scientific Methodology (ISEM), 90146 Palermo, Italy; ignazio.licata3@gmail.com or ignazio.licata@ejtp.info
8 School of Advanced International Studies on Theoretical and Nonlinear Methodologies of Physics, I-70124 Bari, Italy
9 International Institute for Applicable Mathematics and Information Sciences (IIAMIS), B.M. Birla Science Centre, Adarsh Nagar, Hyderabad 500463, India
10 Swedish Institute of Space Physics, Ångström Laboratory, P. O. Box 537, SE-75121 Uppsala, Sweden
* Correspondence: bt@irfu.se

Received: 20 July 2017; Accepted: 29 August 2017; Published: 31 August 2017

Abstract: Background: The Hawking–Perry–Strominger (HPS) work states a new controversial idea about the black hole (BH) information paradox , where BHs maximally entropize and encode information in their event horizon area , with no "hair" thought to reveal information outside but angular momentum, mass, and electric charge only in a unique quantum gravity (QG) vacuum state. New conservation laws of gravitation and electromagnetism , appear to generate different QG vacua, preserving more information in soft photon/graviton hair implants. We find that BH photon hair implants can encode orbital angular momentum (OAM) and vorticity of the electromagnetic (EM) field. Methods: Numerical simulations are used to plot an EM field with OAM emitted by a set of dipolar currents together with the soft photon field they induce. The analytical results confirm that the soft photon hair implant carries OAM and vorticity. Results: a set of charges and currents generating real EM fields with precise values of OAM induce a "curly", twisted, soft-hair implant on the BH with vorticity and OAM increased by one unit with respect to the initial real field. Conclusions: Soft photon implants can be spatially shaped ad hoc, encoding structured and densely organized information on the event horizon.

Keywords: electromagnetic vorticity; electromagnetic orbital angular momentum; black holes; soft photons

1. Introduction

The black hole (BH) information paradox, information loss, and the no-hair theorem were mainly based on the supposed unicity of the quantum gravity vacuum that revealed outside only the macroscopical quantities angular momentum, mass, and electric charge. Hawking, Perry, and Strominger [1] proposed a change to this scenario [2–9], applying new results from general relativity (GR) and quantum gravity (QG): new invariants and symmetries such as supertranslations [10–12] and superrotations [13] with expected observable effects [14–16]. Anyway, to our knowledge, it is still an open question whether Hawking–Perry–Strominger (HPS) soft hair can actually account for the Bekenstein–Hawking entropy and capture the information of black hole microstates.

When one also includes the set of conserved quantities of the electromagnetic (EM) field in this scenario [11,17–19], EM analogs of the supertranslation charges are introduced as a generalization of the electric charge conservation principle. Additonally, in this case, HPS suggest that the unicity of the QG vacuum state is invalidated because of the creation or annihilation of actual physical quantum zero-energy state particles (soft photons). Thus, when EM phenomena are included, BHs are expected to carry a soft electric hair implant, built with soft photons that store information of any process in the event horizon. These soft photons create different QG vacuum states, and because of this, different BHs that have identical macroscopical parameters.

Consider the metric obtained by the collapse of neutral matter at advanced time $v = 0$,

$$ds^2 = -\left(1 - \frac{2M\Theta(v)}{r}\right) dv^2 + 2dvdr + 2r^2\gamma_{z\bar{z}}dzd\bar{z}, \tag{1}$$

written in terms of the round metric $\gamma_{z\bar{z}}$ on the unit sphere S^2 in complex coordinates $(v, r, z, \bar{z})$, where $v = t + r$ and r the radial coordinate, $z = \tan(\phi/2)\exp(-i\theta)$ and $z = 1/\bar{z}$, M the BH mass and $\Theta = 0$ before the shell at $v = 0$ and $\Theta = 1$ after the shell at $v = 0$. The complete information is stored in the S^2 future boundary of the horizon, $\mathcal{H}^+$ of the BH horizon, H, a holographic plate made of quantum pixels whose excitation corresponds to the creation of a spatially localized soft photon on the event horizon with polarization vector $\epsilon_{jm}(\sigma) \propto \partial_z Y_{jm}(z, \bar{z})$ when, for example, a null shock wave with divergence-free charge current carrying an angular momentum eigenstate j is falling into the BH at $v = v_0 > 0$,

$$j^*_v = \frac{Y_{jm}(z, \bar{z})}{r^2}\delta(v - v_0)\,, \tag{2}$$

generating a multipolar radiation field

$$F_{\text{soft}} = \int_{-\infty}^{+\infty} dv F^{(0)}_{zv} = -\frac{e^2}{j(j+1)}\partial_z Y_{jm}\,, \tag{3}$$

where $F^{(0)}$ indicates the photon term of the field and Y_{jm} are spherical harmonics [1]. A suitable combination of falling charges is thus expected to induce a soft electric hair implant characterized by a precise spherical harmonics distribution that describes the invariants of the EM field involved.

In any case, one should obtain observable differences between macroscopically equal BHs, but with different QG vacua. A generic non-trivial asymptotic supertranslation/superrotation (or even electromagnetic) field given by an arbitrary combination of spherical harmonics is expected to modify the spacetime in Equation (1) as proposed by Compére [15]. This metric is valid at future null infinity that follows from a Vaidya metric (which is instead valid everywhere except at future null infinity), and to our knowledge, it is still not proven whether the modified metric by Compére is not just diffeomorphic to a standard metric. The closest proof of that was given by HPS by computing the superrotation charge of a supertranslated metric at future null infinity [20]. In any case, one expects that the measurement of modification of the spacetime metrics is expected from experiments. In the case of Compére's spacetime, one must account for the effects of the whole sphere around the BH such as an array of rulers around the central object or by deviations from closed null geodesics in strong lensing effects. The simple bending of light of a distant star in a finite solid angular range outside of the supertranslation horizon remains unaffected by supertranslations.

For the EM field, Strominger suggested that charged matter generates an asymptotic long-range EM field that can be interpreted as a soft charge. This means that only the long-range field, its value, and its fundamental properties such as vorticity, polarization, and orbital angular momentum are determined by the long time dynamics of the charged matter at times when matter is still very far away from the interaction region or from the event horizon in the case of infall into a BH. Of course, fields produced by infalling matter close to the black hole cannot be associated to soft photons or soft hair. In this case, currents of charged particles that generate EM fields carrying orbital angular momentum and with a characteristic spatial structure and vorticity are expected to produce a soft photon implant with similar characteristics. These properties are independent of the frequency of any real photon considered, as the invariants considered here do not depend strictly on the frequency of the field. This means that the field properties also remain valid in the limit of the null frequency of soft photons, as expected for Hawking, Perry, and Strominger.

Consider the conserved quantity total angular momentum **J** of a particle. This quantity can be decomposed in spin angular momentum (SAM), **S**, related to polarization, and orbital angular momentum (OAM), **L**.

Whilst the splitting of the total angular momentum in two observables, $\mathbf{J} = \mathbf{L} + \mathbf{S}$, is valid for massive particles, it does not always have a precise physical meaning for the EM field and for the photon; in any case, SAM and OAM are auxiliary concepts that describe the photon wavefunction properties with respect to rotations, and OAM gives the order of the spherical functions involved in the radiation field together with the parity of the photon state, following precise rules for the composition of **L** and **S** from the classical field formulation [21–23] down to the single photon level, where intensity corresponds to the probability of generating a photon in a specific region of spacetime [24–26]. In contrast to plane waves (which carry linear momentum with no azimuthal component), those fields can have nonzero total azimuthal momentum p_ϕ but an identically zero azimuthal component of linear momentum [27]. EM-OAM is currently applied in many research fields [28] and technologies: quantum and classical communications [29–31], astrophysics [32], and nanotechnology. Prototype examples of fields carrying specific SAM and OAM eigenvalues are Laguerre–Gaussian (LG) modes that provide an orthogonal fundamental basis to expand any OAM field and present a well-known spatial structure in intensity and phase distributions. They represent cylindrically symmetric structured EM beams that carry $l\hbar$ OAM per photon relative to their symmetry axis with amplitude, in cylindrical coordinates (r, φ, z),

$$u_{lm}^{L-G}(r,\varphi,z) = \sqrt{\frac{2m!}{\pi(m+l)!}}\frac{1}{w(z)}\left[\frac{r\sqrt{2}}{w(z)}\right]^{l} L_m^l\left[\frac{2r^2}{w^2(z)}\right] e^{\frac{-r^2}{w(z)^2}-\frac{\mathrm{i}kr^2}{2R(z)}} e^{-\mathrm{i}(2m+l+1)\arctan\left(\frac{z}{z_R}\right)} e^{-\mathrm{i}l\varphi} \tag{4}$$

where z_R is the Rayleigh range of the beam, $w(z)$ the beam waist, $L_m^l(x)$ the associated Laguerre polynomial, and $R(z)$ the curvature radius. The azimuthal and radial indices l and m give the OAM and the number of radial nodes of the associated intensity profile, respectively [18,22], with a precise spatial structure (Generally, all fields carry energy, linear momentum, and orbital angular momentum [33]. The EM field is a vector field and therefore carries both spin and orbital angular momentum. These observables are emitted in the form of volumetric densities [19], and therefore cannot be measured at a single point but must be integrated/averaged over a finite (possibly very small) volume—for instance, the volume occupied by a sensor).

Any generic field can be written as a superposition of LG modes shown in Equation (4) and decomposed into multipolar fields, spherical harmonics, and in terms of paraxial fields that depend only on the wavelength or frequency chosen [34]. Additionally, soft photon hair implants can be written in terms of LG modes, and in certain cases can actually have the properties of a single LG mode, characterized by its precise spatial structure and OAM state. It is noteworthy that these properties remain valid down to the single photon level.

The bridge between Equations (2) and (3) that describe the multipolar distribution of soft photon hair implants and LG modes starts from a simple LG beam with $m = 0$. In this case, the vector potential $\vec{A}$ in terms of multipolar superpositions of circularly polarized plane waves is

$$\vec{A} = 2\pi \sum_{j=\|l+p\|}^{\infty} i^j (2j+1)^{1/2} C_{jlp} \left[\vec{A}_{j\,(l+p)}^{(\mathrm{m})} + i\vec{A}_{j\,(l+p)}^{(\mathrm{e})}\right] \tag{5}$$

and

$$C_{jlp} = \sqrt{\frac{(j+p)!(j-p)!(j+l+p)!(j-l-p)!}{(j-\frac{|l|-|l+2p|}{2})!}} k(-)^{j+\frac{l+|l+2p|}{2}} 2^{|l|/2+1} w_0^{-2j-1+|l+2p|} L_{j-\frac{|l|+|l+2p|}{2}}^{|l+2p|} \left((w_0/k)^2\right) , \quad (6)$$

where the vector potential $\vec{A}$ is decomposed in the magnetic (m) and electric (e) terms, k is the wavenumber, w_0 the waist of the associated Gaussian beam, and L_l^p is the associated Laguerre polynomial. This field is composed of multipolar solutions with different total angular momenta, but with the same projection of the angular momentum in the direction z, which is $+1$ or -1 depending on the polarization of the field and $(j, m = l + p)$, p represents the circular polarization operator and k the wavevector. LG modes with OAM l and polarization p present multipolar modes with a fixed component $m = l + p$ along z of the angular momentum [35].

2. Results

Currents generate EM fields and radiation with well-defined patterns, polarization, related to the spin angular momentum of the photon (SAM), the orbital angular momentum, and in this case, soft photon implants. Are there similarities between the two fields as one could expect, or are the two fields simply equal but for the $\nu \to 0$ frequency expected for soft photons? What are the field properties which are preserved?

In this section, we address these questions by calculating the standard field generated by a given set of multipolar sources, and then we compare the results of our numerical simulation with the numerical results that describe the soft photon implant expected from the same set of charges that is described by Equations (2) and (3).

Superpositions of multipolar sources generated by an arbitrary distribution of charges and currents j_v^* in a finite source volume V' can generate spatially-structured EM fields that carry a precise combination of OAM states and spherical harmonics (or an equivalent combination of LG modes) with respect to a given point in spacetime. For the sake of simplicity, we now consider fields that are characterized by a precise phase structure in space with a precise spectrum of OAM values. The field is obtained independently from the radiating system, as angular momentum and its volumetric density is a property of the field emitted by any radiation, not the property of the radiator itself, and is independent of the frequency and spatial dimensions in the ideal case [18,22,23,36].

In the numerical simulations, we use as example a realistic distribution of dipolar currents in a set of azimuthally-dephased radiating dipoles on a circle with radius r_c and center O_c that produce a radiating EM field with a well-defined OAM value l and a well-defined distribution of spherical harmonics. This set of dipoles has a spatial extension much smaller than the wavelength emitted, $d = \lambda/100$, and are azimuthally dephased of $\delta\varphi = \pi/4$ to generate an EM field with $l = 1$ OAM value calculated with respect to the center of symmetry of the dipole array with linear polarization across the $x^1 = x$ axis of the new accelerated local frame (x^i). The circle hosting the currents is orthogonal to the direction $r_\perp$ connecting 0_c and the center of the BH far away from the BH event horizon and in far field conditions.

We assume that the BH radius, r^*, is $r^* \gg r_c$ and approximate the metrics (valid also near the horizon $r \sim 2MG$) in a small angular region $\theta = 0$, where a small neighborhood of an observer can be described in first approximation as a Rindler coordinate system and a set of observers on the direction $r_\perp$ identify—at a first approximation—a class of Rindler observers. For these observers and with the approximations here adopted, the radiating field from the currents is not significantly affected by the free-fall radiating process [37,38] neglected in first approximation.

Let us now consider the onset of a soft photon hair implant from these multipolar sources, as charged matter generates an asymptotic long-range EM field that can be interpreted as a soft charge. We calculate the spatial distribution of the soft photon implant from Equations (2) and (3) in a neighborhood of the observation point O.

The results are reported in Figure 1, which depicts the real and soft photon hair implant induced by four falling dipolar currents distributed on a circle with radius $r_c = \lambda/10$. The upper panels of Figure 1 show the probability of emission of a photon in a superposition of OAM states and the spatial phase distribution of the EM field calculated in a window of $25\lambda \times 25\lambda$. The point of observation of the field is located far away from the charges, at 300 wavelengths distance in the direction $r_\perp$, in far field conditions.

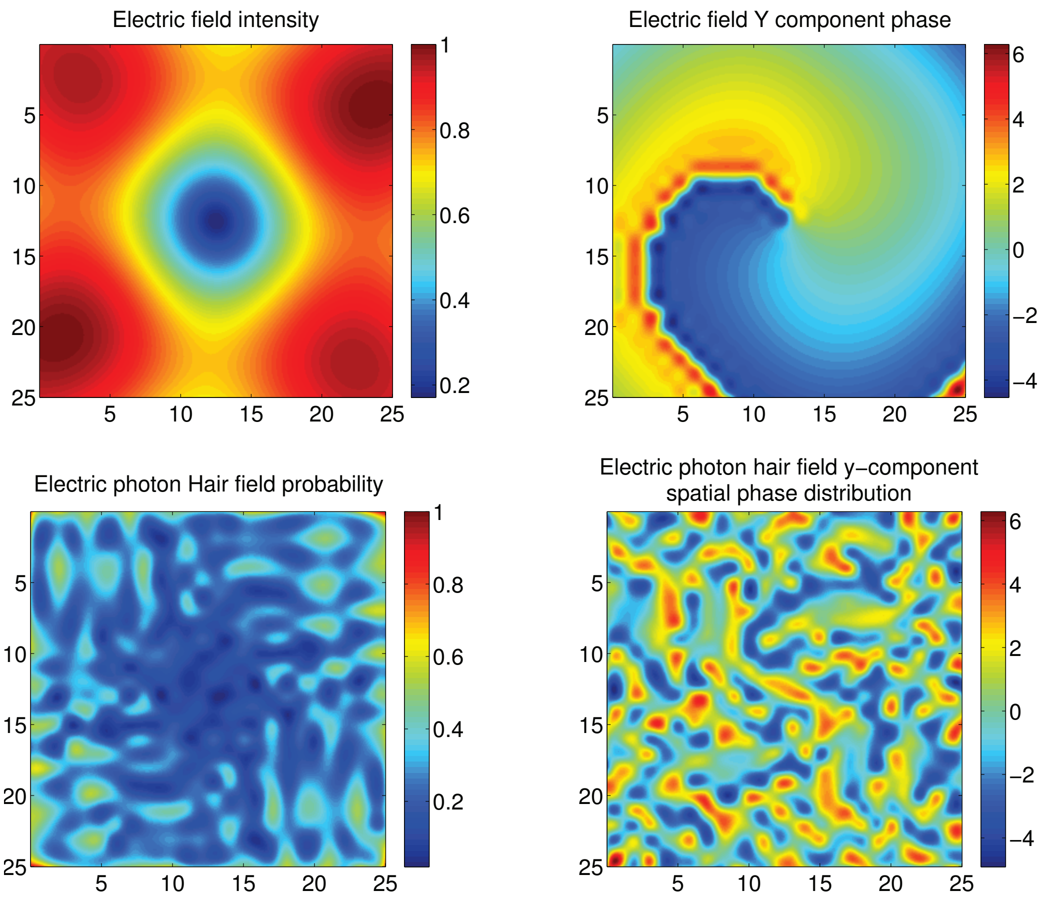

Figure 1. Normalized electric field (E) probability of photon emission (intensity) and phase distribution of an $l = 1$ vortex generated by four dipoles oriented across the y-axis (upper panel). The four dipoles—much smaller than λ—are distributed on a circle with radius $\lambda/10$. In the lower panel we find the probability of associating a soft photon hair in the soft photon implant and the spatial phase information generated by these currents. Units are in λ, and the field properties also remain valid for any frequency when $\nu \to 0$.

The lower panels show the probability of associating a soft photon (with zero frequency) in the corresponding hair implant and the corresponding phase profile, after neglecting the backreaction of the shell and of the EM field on the geometry.

All numerical simulations were performed with Matlab and NEC (Numerical Electromagnetics Code) [39–41] that morphed the standard NEC input and output into the correct shape of the static spacetime geometry here considered through a geometrical optics transformation from analog gravity [42,43].

Owing to the realistic simulation of the four dipole currents, the spiral spectrum [44] of the electric field component along x generated by the set of dipoles clearly shows a complex structure of OAM components where the dominant term is $l = 1$ (Figure 2).

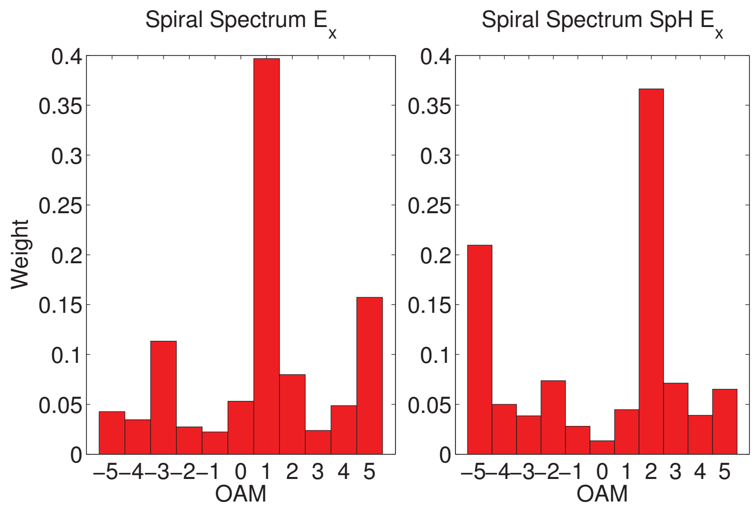

Figure 2. (**Left**): spiral spectrum of the radiation field emitted by the dipolar currents shows a dominant contribution of the $l = 1$ vorticity of the source; (**Right**): spiral spectrum of the soft photon field is peaked on a dominant value ($l = 2$), which is one unit larger that the orbital angular momentum (OAM) peak of the real photon field.

We see that soft photon implants can exhibit organized spatial structures like the original field, but the two fields present different spatial structures and vorticity is preserved: the numerical results show that the spiral spectrum of the EM field generated by the four falling dipoles—peaked at $l = +1$—has similarities to that of the soft photon hair implant but for a translation of the peak to $l = +2$, apparently preserving the spatial information of the real photon field.

Naively, this effect of spiral spectrum shift finds an interesting parallelism with the optical experiments involving OAM beams: the soft photon hair implant F_{soft} behaves as if it were the product of the initial radiation field of the current j_v^* after crossing a single-bifurcation fork hologram—a phase modulating device—that shifts the spiral spectrum by one OAM unit [22], and ideally shifts the frequency to zero as expected for a soft photon.

The shift of the spiral spectrum observed in the soft photon implant with respect to the real field emitted by the falling currents can find a mathematical explanation as follows: consider a set of charges that radiate an EM field described by a single ideal LG mode with a given topological charge l as in Equation (4). This field is characterized by its polarization state and a finite value of OAM (both SAM—related to polarization—and OAM form the invariant EM total angular momentum) and with a precise spatial structure in intensity and phase. The decomposition of this field in spherical modes puts in immediate evidence the angular momentum properties through the eigenfunctions of the angular momentum operators, Y_{jm} being the eigenfunction of the operators J^2 and J_z, where z in this case is $r_\perp$. By applying Equation (3) and the derivation rules in the Riemann sphere [45,46], after some algebra, being

$$\frac{d}{dx} L_k^l = -L_{k-1}^{l+1}, \tag{7}$$

where l and k are two arbitrary indexes, it is clear that the resulting soft photon field presents terms with increased OAM values of exactly one unit (adding an $l = 1$ value to the initial OAM value of the field) with respect to that of the real field emitted by the infalling currents in Equations (5) and (6), confirming our numerical findings in the spiral spectra.

In this way, we provide a novel physical interpretation to the *lush head* of BHs "soft hair" that can carry OAM in a modified spacetime with increased OAM value and with an organized spatial structure and phase spatial structure that are derived from the fields of the "real" photons. This means that information encoded in the field properties such as vorticity are preserved with a modification in the orbital angular momentum spectrum.

3. Conclusions

Following HPS, charged matter generates an asymptotic long-range EM field that can be interpreted as a soft charge. Black holes appear to encode the spatial information of these currents generating OAM beams in twisted hair implants that present a local a spatial structure on the event horizon. All EM information is encoded and determined by the long time dynamics of the charged matter, very far away from the interaction region, or away from the black hole event horizon, in the case of infall.

We have shown that we can use the spatial symmetries of EM fields to generate organized local spatial structures on soft photon implants and encode structured and densely organized information on the event horizon. In fact, when charges generating structured fields fall in the BH gravitational field, accounting for the gravitational memory effect, they are expected to generate organized structures of soft photons but result different from those of the "real" photons. It is noteworthy that the OAM content of the soft photon hair implant is characterized by its OAM state distribution peaked on a value higher than that of the real EM field emitted by the infalling currents.

BHs can have "curly", twisted, structured EM soft-hair implants where information can be written onto the horizon in an organized way. This procedure can be extended to more complex field configurations expressed in terms of conserved quantities and symmetries with additional supertranslation fields.

Acknowledgments: Fabrizio Tamburini gratefully acknowledges the financial support from ZKM and MSC-BW. Mariafelicia De Laurentis is supported by ERC Synergy Grant "BlackHoleCam" Imaging the Event Horizon of Black Holes awarded by the ERC in 2013 (Grant No. 610058). All the authors acknowledge M.V. Licata for the help during the revision of the manuscript.

Author Contributions: Fabrizio Tamburini, Mariafelicia De Laurentis, Ignazio Licata and Bo Thidé discussed the main idea; Fabrizio Tamburini performed the numerical simulations and developed the analytical method; All the authors contributed in the writing of the paper.

Conflicts of Interest: The authors declare no conflict of interest.

References

1. Hawking, S.W.; Perry, M.J.; Strominger, A. Soft hair on black holes. *Phys. Rev. Lett.* **2016**, *116*, 231301.
2. Hawking, S.W. Black hole explosions. *Nature* **1974**, *248*, 30–31.
3. Hawking, S.W. Particle creation by black holes. *Commun. Math. Phys.* **1975**, *43*, 199–220.
4. Hawking, S.W. Breakdown of predictability in gravitational collapse. *Phys. Rev. D* **1976**, *14*, 2460.
5. Page, D. Hawking radiation and black hole thermodynamics. *New J. Phys.* **2005**, *7*, 203.
6. Bekenstein, J.D. Black holes and entropy. *Phys. Rev. D* **1973**, *7*, 2333.
7. Bardeen, J.M.; Carter, B.; Hawking, S.W. The four laws of black hole mechanics. *Commun. Math. Phys.* **1973**, *31*, 161–170.
8. Misner, C.W.; Thorne, K.S.; Wheeler, J.A. *Gravitation*; W. H. Freeman: San Francisco, CA, USA, 1973.
9. Chandrasekhar, S. *The Mathematical Theory of Black Holes*; Oxford University Press: New York, NY, USA, 1992.
10. Strominger, A. On BMS invariance of gravitational scattering. *J. High Energy Phys.* **2014**, *2014*, 152.
11. Mitra, T.; He, P.; Porfyriadis, A.P.; Strominger, A. New symmetries of massless QED. *J. High Energy Phys.* **2014**, *2014*, 112.
12. Bondi, H.; van der Burg, M.G.J.; Metzner, A.W.K. Gravitational waves in general relativity. VII. Waves from axi-symmetric isolated systems. *Proc. R. Soc. Lond. A* **1962**, *269*, 21–52.
13. Donnay, L.; Giribet, G.; Gonzalez, H.A.; Pino, M. Supertranslations and superrotations at the black hole horizon. *Phys. Rev. Lett.* **2016**, *116*, 091101.
14. Mirbabayi, M.; Porrati, M. Dressed hard states and black hole soft hair. *Phys. Rev. Lett.* **2016**, *117*, 211301.
15. Compére, G. Bulk supertranslation memories: A concept reshaping the vacua and black holes of general relativity. *Int. J. Mod. Phys.* **2016**, *D25*, 1644006.

16. Sheikh-Jabbari, M.M. Residual diffeomorphisms and symplectic soft hairs: The need to refine strict statement of equivalence principle. *Int. J. Mod. Phys.* **2016**, *25*, 1644019.
17. Fushchich, V.I.; Nikitin, A.G. *Symmetries of Maxwell's Equations*; D. Reidel Publishing Company: Dordrecht, Holland, 1987.
18. Thidé, B. *Electromagnetic Field Theory*, 2nd ed.; Dover Publications, Inc.: Mineola, NY, USA, 2011, in press.
19. Thidé, B.; Tamburini, F.; Then, H.; Someda, C.G.; Ravanelli, R.A. The physics of angular momentum radio. *arXiv* **2014**, arXiv:1410.4268.
20. Hawking, S.W.; Perry, M.J.; Strominger, A. Superrotation charge and supertranslation hair on black holes. *High Energy Phys.* **2017**, *2017*, 1–33.
21. Andrews, D.L. *Structured Light and Its Applications: An Introduction to Phase-Structured Beams and Nanoscale Optical Forces*; Academic Press: San Diego, CA, USA, 2011.
22. Torres, P.; Torner, J.L. (Eds.) *Twisted Photons: Applications of Light with Orbital Angular Momentum*; Wiley-VCH Verlag GmbH & Co. KGaA: Weinheim, Germany, 2011.
23. Jackson, J.D. *Classical Electrodynamics*, 3rd ed.; John Wiley & Sons, Inc.: New York, NY, USA, 1999.
24. Leach, J.; Padgett, M.J.; Barnett, S.M.; Franke-Arnold, S.; Courtial, J. Measuring the orbital angular momentum of a single photon. *Phys. Rev. Lett.* **2002**, *88*, 257901.
25. Calvo, G.F.; Picòn, A.; Bagan, E. Quantum field theory of photons with orbital angular momentum. *Phys. Rev. A* **2006**, *73*, 013805.
26. Tamburini, F.; Vicino, D. Photon wave function: A covariant formulation and equivalence with QED. *Phys. Rev. A*, **2008**, *78*, 052116.
27. Speirits, F.C.; Barnett, S.M. Do waves carrying orbital angular momentum possess azimuthal linear momentum? *Phys. Rev. Lett.* **2013**, *111*, 103602.
28. Grier, D.G. A revolution in optical manipulation. *Nature* **2003**, *424*, 810–816.
29. Mair, A.; Vaziri, A.; Weihs, G.; Zeilinger, A. Entanglement of the orbital angular momentum states of photons. *Nature* **2001**, *412*, 313–316.
30. Tamburini, F.; Mari, E.; Sponselli, A.; Thidé, B.; Bianchini, A.; Romanato, F. Encoding many channels on the same frequency through radio vorticity: first experimental test. *New J. Phys.* **2012**, *14*, 033001.
31. Wang, J.; Yang, J.Y.; Fazal, I.M.; Ahmed, N.; Yan, Y.; Huang, H.; Ren, Y.; Yue, Y.; Dolinar, S.; Tur, M.; et al. Terabit free-space data transmission employing orbital angular momentum multiplexing. *Nat. Photonics* **2012**, *6*, 488–496.
32. Tamburini, F.; Thidé, B.; Molina-Terriza, G.; Anzolin, G. Twisting of light around rotating black holes. *Nat. Phys.* **2011**, *7*, 195–197.
33. Soper, D.E. *Classical Field Theory*; John Wiley & Sons, Inc.: New York, NY, USA, 1976.
34. Rose, M.E. *Elementary Theory of Angular Momentum*; Dover Publications, Inc.: New York, NY, USA, 1995.
35. Molina-Terriza, G. Determination of the total angular momentum of a paraxial beam. *Phys. Rev. A* **2008**, *78*, 053819.
36. Thidé, B.; Then, H.; Sjöholm, J.; Palmer, K.; Bergman, J.; Carozzi, T.D.; Istomin, Y.N.; Ibragimov, N.H.; Khamitova, R. Utilization of photon orbital angular momentum in the low-frequency radio domain. *Phys. Rev. Lett.* **2007**, *99*, 087701.
37. Rindler, W. *Essential Relativity*; Van Nostrand Reinhold Co.: New York, NY, USA, 1969.
38. De Almeida, C.; Saa, A. The radiation of a uniformly accelerated charge is beyond the horizon: A simple derivation. *Am. J. Phys.* **2006**, *74*, 154–158.
39. Burke, G.; Poggio, A. *NEC Part I: Program Description—Theory, Technical Report Lawrence Livermore Laboratory*; 1981. Available online: http://www.radio-bip.qc.ca/NEC2/nec2prt1.pdf (accessed on 30 August 2017).
40. Burke, G.; Poggio, A. *NEC Part II: Program Description—Code, Technical Report Lawrence Livermore Laboratory*; 1981. Available online: http://www.radio-bip.qc.ca/NEC2/nec2prt2.pdf (accessed on 30 August 2017).
41. Burke, G.; Poggio, A. *NEC Part I: Program Description—User's Guide, Technical Report Lawrence Livermore Laboratory*; 1992. Available online: http://www.radio-bip.qc.ca/NEC2/nec2prt3.pdf (accessed on 30 August 2017).
42. Landau, L.D.; Lifshitz, E.M. The Classical Theory of Fields. In *Course of Theoretical Physics*; Elsevier: Pergamon, Turkey; Oxford, UK, 1975; Volume 2.
43. Barcelo, C.; Liberati, S.; Visser, M. Analogue Gravity. *Living Rev. Relativ.* **2011**, *14*, 3.
44. Torner, L.; Torres, J.; Carrasco, S. Digital spiral imaging. *Opt. Express* **2005**, *13*, 873–881.

45. Abramowitz, M.; Stegun, I.A. (Eds.) *Handbook of Mathematical Functions with Formulas, Graphs, and Mathematical Tables*, 9th printing; Dover: New York, NY, USA, 1972; p. 17.
46. Arfken, G. *Mathematical Methods for Physicists*, 3rd ed.; Academic Press: Orlando, FL, USA, 1985.